International Journal of Physics
and Research (IJPR)
ISSN(P): 2250-0030; ISSN(E): 2319-4499
Vol. 3, Issue 5, Dec 2013, 51-60

INFLUENCE OF IN AND SE ADDITION ON THE MECHANICAL PROPERTIES OF SN-5SB-2CU BEARING ALLOYS

RIZK MOSTAFA SHALABY[1] & MUSTAFA KAMAL[2]

[1,2]Metal Physics Laboratory, Physics Department, Faculty of Science, Mansoura University, Mansoura, Egypt

[1]Physics Department, Faculty of Science and Arts, Al Jouf University, Al-Qurayat, Saudi Arabia

ABSTRACT

Effects of Se or In addition at 2 wt. % on mechanical properties of melt-spun Sn-5Sb-2Cu lead free bearing solder alloys were investigated and analyzed. The near peritectic Sn-5Sb bearing solder alloy has considerable attention for high temperature electronic applications, especially on step soldering technology and flip-chip connection. This study revealed that the structure of Sn-5Sb-2Cu is characterized by the presence of new intermetallic compounds (IMCs) of $Sb_{0.021}Sn_{0.79}$, Cu_3Sb and Cu_3Sn particles within β-Sn matrix. The quaternary Sn-5Sb-2Cu-2In alloy exhibit additional constituent phases of new IMC InSb for Sn-5Sb-2Cu-2In. For penta Sn-5Sb-2Cu-2Se-2In alloy, extra peaks of cubic InSb intermetallic compound of space group F-43m were found in addition to $Sb_{0.021}Sn_{0.79}$, Cu_3Sb and Cu_3Sn precipitates are distributed in the β-Sn matrix. This study revealed that the melt-spun Sn-5Sb-2Cu-2Se-2In alloy have higher creep resistance and mechanical properties compared with the other three alloys. The prime concentration during the study was on the role of new intermetallic compounds on the creep resistance and mechanical properties.

KEYWORDS: Bearing Alloys, Mechanical Properties, Intermetallic Compounds, Indentation Creep

INTRODUCTION

The near peritectic Sn-5Sb Pb-free solder alloy has received considerable attention for high temperature electronic applications, especially on step soldering technology, flip chip connection [1-3], solder ball connections and bonding a semiconductor device onto a substrate. Antimony has also been used as the alloying element in the tin-based systems to provide suitable substitutes for Sn-Pb solder alloys. One of these materials is the near-peritectic composition Sn-5Sb, with a melting point of 245˚C [4]. Solders in joints usually work at high homologous temperature because of their low melting temperature. In this temperature range, creep is the most important deformation mechanism, and the stress and strain concentrations at the solder joints must be effectively relaxed by creep to guarantee the solder joint reliability [5]. Accordingly, the creep study of tin-antimony alloys has received a great deal of attention [4, 6, 7]. The indentation creep process can be defined as the time dependent penetration of a hard indenter into the material under constant load and temperature. The variation in the indentation size, expressed either as a change in diagonal length (Vickers test), is monitored with dwell time. Thus, the time dependent flow behavior of materials can be studied by these simple hardness tests. This can be particularly advantageous when the material is only available as small test pieces or there are some difficulties with the machining of samples made of very soft materials. Therefore, the indentation creep tests, regarded as a quick, simple and non-destructive procedure to extract information on the mechanical behavior of materials, greatly reduce the effort for sample preparation [8, 9]. Several papers have discussed the impression creep behavior or indentation creep study of lead-free Sn-5% Sb solder alloy [10-12]. The microstructure of Sn-Sb alloys however is quite different from of Pb-Sn solders. In Pb-Sn solders, lamellar and degenerate lamellar microstructures are often formed [13]. In Sn-Sb alloys with high concentration of Sb, dispersion of intermetallics such as SbSn precipitates are distributed within the matrix.

This provides a significant composite strengthening effect that reduces the creep rate at temperatures below 100 ˚C [14]. The majority of published work has focused on the Sn-5%wt.Sb alloy [15-18]. Lead-free Sn-based alloy systems with different alloying elements such as Ag, Bi, Cu, In, Sb and Zn have been developed and their microstructures, mechanical properties and solderability have been reported [19-21]. Among the developed lead free solders, Sn-Sb alloys are of interest because of their suitable mechanical and creep properties. The improved creep resistance and strength in these alloys have been attributed to the solid solution hardening effects of Sb [4] and formation of SnSb intermettalic particles [6, 10]. In the Sn-Sb alloy system, the near-preitectic Sn-5%Sb alloy, with a melting point of 245 ˚C, has been considered as a potential material having the advantages of good resistance [10, 11, 16, 22] and superior mechanical properties [23]. Separate additions of 3.5 wt.% Ag and 1.5 wt.% Au to the Sn-5Sb base alloy have resulted in enhanced creep resistance , mainly due to the respective formation of Ag_3Sn and $AuSn_4$ intermetallics in the β-Sn matrix[2]. In another work, [24] they have studied indentation creep and mechanical properties of quaternary Sn-10Sb-Cu-2Se based alloy by indentation method at room temperature. They showed that the stress exponent values in the range of 3.93-5.12. El-Daly et al [25] studied the effect of 0.7 %Cu and 0.7%Ag on the tensile creep behavior of the Sn-5Sb alloy. They showed that both Ag and Cu refined the microstructure and formed new intermetallic compounds. Addition of Cu which resulted in the formation of Cu_6Sn_5 particles was found to be more effective than Ag in decreasing the creep rate and increasing creep resistance of the base material. Recently, creep behavior of Sn-10Sb-2Cu based alloy with separate additions of 2%Pb, Se, Cd, Zn and Ag has been studied by indentation method at room temperature [24]. The obtained stress exponent values in the range of 3.4-5.1 have been found to be in good agreement with the values of Sn-Sb reported in the literature. There have been many attempts to investigate the possibility of gaining information on creep properties of solder alloys by the use of impression tests [26-29]. Impression creep, developed by Chu and Li [30], is a unique method for determining creep behavior of materials [31].This test involves applying a constant load to a flat-ended cylindrical punch and recording variations of penetration depth of the indenter as a function of time. This configuration will provide a constant stress condition during the entire creep test period. In contrast to conventional creep tests, which need tensile or compressive specimen, in this method, all creep data can be obtained with a small piece of material. This can particularly be advantageous when the material is only available as small test pieces or there are some difficulties with the machining of samples made of very soft materials such as solder alloys. In the present study, the effects of Se or In on the mechanical and creep properties of Sn-5Sb-2Cu lead free solder alloys at room temperature under bearing conditions were investigated. The results are predicted to gain great prominence in the further development of new bearing solder alloys for different electronic packaging applications. However, the most interesting application of the rapid solidification technique is the synthesis of new alloy phases, which cannot be obtained either under equilibrium conditions or by quenching from the solid state.

EXPERIMENTAL PROCEDURES

Materials and Processing

The four alloys used in this investigation were Sn-5 wt.% Sb-2 wt.% Cu, Sn-5 wt.% Sb-2 wt.% Cu-2 wt.% Se, Sn-5 wt.% Sb-2 wt.% Cu-2 wt.% In and Sn-5 wt.% Sb-2 wt.% Cu-2 wt.% Se-2 wt.% In. The lead free bearing solders were prepared from high purity tin, antimony, copper, selenium and indium better than 99.9 %. The process of melting was carried out in electrical muffle furnace and melted at 600 ˚C. The melt was hold at 600 ˚C for 1 h to complete the dissolution of Sn, Sb, Cu, Se and In and then poured in a porcelain crucible to prepare long ribbon. Long ribbons of about 4 mm width and ≈ 60-100 μm thickness were prepared by a single roller method in air by melt spinning technique. The surface velocity of the roller was 31.4 m/s giving high cooling rate. The elastic moduli were determined using the

dynamic resonance method. The values of the dynamic Young's modulus, E and internal friction,Q^{-1} were calculated using the dynamic resonance from the relationship [32, 33]:

$$E = 38.32 \frac{\rho L^4 f_0^2}{d^2} \quad (1)$$

$$Q^{-1} = 0.5773 \frac{\Delta f}{f_0} \quad (2)$$

Where ρ the density of the sample test, L is the length of the vibrated part of the melt-spun ribbon, f_0 is the resonance frequency of the sample and d is the sample's thickness. In particular, bulk modulus, B and shear modulus, G may be estimated from the Young's modulus E and Poisson's ratio, σ:

$$B = \frac{E}{3(1-2\sigma)} \quad (3)$$

$$G = \frac{E}{2(1+\sigma)} \quad (4)$$

The structure of these alloys was examined by x-ray diffraction (XRD, X pert PRO, PANalytical using CuK_α target with secondary monochromator).

Indentation Creep Tests

The details of the testing arrangement are explained elsewhere [34] and would be only briefly presented here. Each polished specimen was tested in a Vickers hardness tester where the applied load and testing time were the only variables. Vickers test uses a diamond pyramid with square base and the Vickers hardness number is given by $H_v=0.185F/d^2$, where F is the applied load in N and d is the average diagonal length in mm. Indentation creep measurements of used samples was studied by Vickers micro-hardness tester (mode-FM-7 Japan) were made on each sample using 10, 25 and 50 gf load for dwell time up to 99 s. Each reading was an average of at least 15 separate measurements taken at random places on the surface of the specimens. Among the various techniques such as Sargent-Ashby and Mulhearn-Tabor the analysis of the indentation creep was carried out using the technique employed by Mulhearn-Tabor [35] as it was found to be the most suitable method for the current work:

$$-\left(n+\frac{1}{2}\right)\log H_v = \log t + B \quad (5)$$

H_v is the Vickers number, t is the indentation dwell time and B is the constant. If hardness is plotted versus dwell time on log-log scale, a straight line with slope – (n+1/2) is obtained.

RESULTS AND DISCUSSIONS

X-Ray Diffractometry Analysis

X-ray diffraction analysis was performed to determine the phase composition of the IMCs particles in the four melt spun Sn-5Sb-2Cu, Sn-5Sb-2Cu-2Se, Sn-5Sb-2Cu-2In and Sn-5Sb-2Cu-2Se-2In melt-spun alloys. As can be seen in Figure 1, all the four melt-spun alloys are mainly composed of peaks indexed to a tetragonal cell of Sn with a=0.5857 and c=0.317 nm and precipitated $Sb_{0.21}Sn_{0.79}$, Cu_3Sn and Cu_3Sb IMCs. The addition of Cu to the Sn-5Sb can result in the formation $Sb_{0.21}Sn_{0.79}$, Cu_3Sn and Cu_3Sb precipitates. However, the Cu selectively combines with Sn, and Sb to form a Cu-Sn and Cu-Sb. The IMC InSb phase was found in the XRD pattern of Sn-5Sb-2Cu-2In and Sn-5Sb-5Sb-2Se-2In alloys,

indicating the successful alloying of Sb and in after the melting process. Therefore, it is concluded that rapid solidification leads to the formation of new inter-metallic compounds $Sb_{0.21}Sn_{0.79}$ (tetragonal), Cu_3Sb, Cu_3Sn and InSb (cubic) which were not formed by the conventional method. The hkl of InSb for Sn-5Sb-2Cu-2In are 111, 220, at 2θ=23.8 and 39.2 respectively. Also, the hkl of InSb phase 1 1 1, 2 2 0, 3 1 1, 3 3 1, 4 2 0, 4 2 2, 5 3 1 at 2θ = 23.77, 39.31, 46.48, 62.5, 64.5, 72.31 and 89.278 respectively for Sn-5Sb-2Cu-2Se-2In alloy. At the same time, the Cu_3Sn and Cu_3Sb phase were formed, which were due to the alloying of Sn with Cu and Sb. Moreover, the relative intensities of β-Sn and $Sb_{0.21}Sn_{0.79}$ were found to be slightly decreased with the addition of Se and in due to the formation of Cu_3Sb and Cu_3Sn phases. Meanwhile, the intensity of the Sn-rich phase decreases for Se addition while it increases for in addition. It is reported that there is almost no solid solubility of Se or In in Sn. The addition of Se and in to the Sn-5Sb-2Cu can result in the formation of increase of InSb inter-metallic compound. It is reported that for Sn-5Sb-2Cu-2Se-2In alloy formation of InSb compound is much higher than that of Cu_3Sb and Cu_3Sb compounds. Thus, the investigated solder systems will form InSb compounds rather $Sb_{0.21}Sn_{0.79}$, Cu_3Sb and Cu_3Sn compounds. Table 1 summarizes the possible corresponding phases and particle size, lattice parameters, and axial ratio (c/a) for β-Sn melt-spun alloy. We found that the axial ratio decreased by the addition for 2 wt. % Se and 2 wt. % in, because of the difference in the atomic diameters of studying elements at room temperature. Table 1 illustrates the ability of alloying elements to refine the particle size of Sn-5Sb-2Cu indicating that Se was significantly stronger than in. However, the addition of Se or in can refined the β-Sn rich phase to some content and developed some new IMCs in the solder matrix. These new phases can be classified into three types; solid solutions extending beyond the equilibrium concentrations, crystalline phases and-non-crystalline phases. Rapid solidification has effects on the structure of the alloys, which are produced by the refinement of the cast particle size.

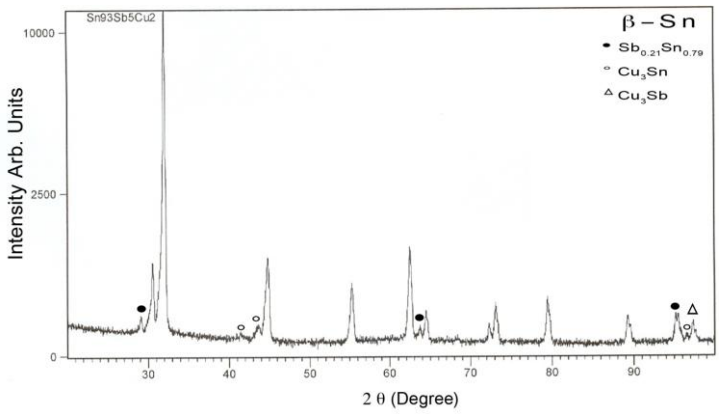

(a)

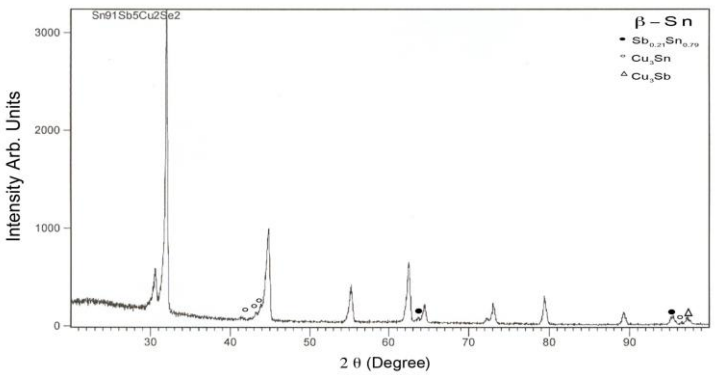

(b)

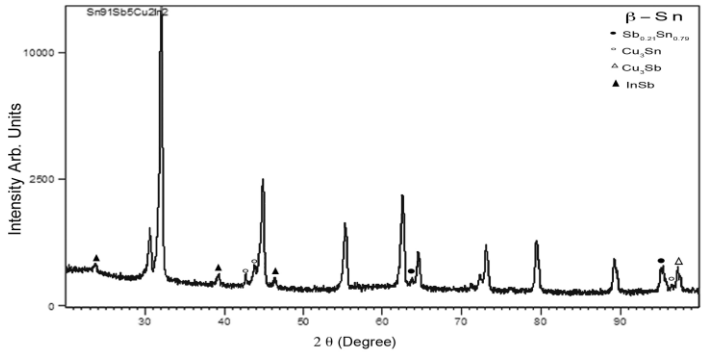

(c)

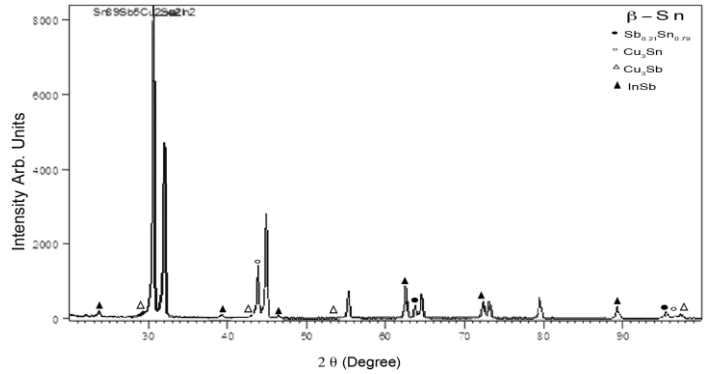

(d)

Figure 1: X-Ray Diffraction of the Rapidly Solidified Sn-5Sb-2Cu Based Lead Free Bearing Solder Alloys, (a) Sn-5Sb-2Cu, (b) Sn-5Sb-2Cu-2Se, (c) Sn-5Sb-2Cu-2In and (d) Sn-5Sb-2Cu-2Se-2In

Table 1: Details of the XRD Analysis

Solder	Phases	Crystal System	Particle Size (nm)	Lattice Parameters		
				a (Å)	c (Å)	c/a
Sn-5Sb-2Cu	β-Sn	Body centered tetragonal	387.39	5.857	3.170	
	$Sb_{0.21}Sn_{0.79}$	Tetragonal	465.26	6.135	3.180	0.542
	Cu_3Sn	Hexagonal	655.02			
	Cu_3Sb	Cubic	785.06	5.996	5.996	
Sn-5Sb-2Cu-2Se	β-Sn	Body centered tetragonal	256.22	5.850	3.179	
	$Sb_{0.21}Sn_{0.79}$	Tetragonal	450.05	6.130	3.185	0.543
	Cu_3Sn	Hexagonal	650.22			
	Cu_3Sb	Cubic	790.23	5.986	5.986	
Sn-5Sb-2Cu-2In	β-Sn	Body centered tetragonal	200.52	5.842	3.181	
	$Sb_{0.21}Sn_{0.79}$	Tetragonal	445.23	6.120	3.187	0.544
	InSb	Cubic	506.50	6.495	6.495	
	Cu_3Sn	Hexagonal	560.26			
	Cu_3Sb	Cubic	620.24	5.975	5.975	
Sn-5Sb-2Cu-2Se-2In	β-Sn	Body centered tetragonal	187.24	5.841	3.183	
	$Sb_{0.21}Sn_{0.79}$	Tetragonal	420.25	6.110	3.191	0.545
	InSb	Cubic	348.02	6.484	6.484	
	Cu_3Sn	Hexagonal	501.01			
	Cu_3Sb	Cubic	584.27	5.965	5.965	

Mechanical Properties

Elastic Moduli Measurements

Adding small amount of third or fourth alloying elements to solders has been found to be an excellent method to improve mechanical properties. The alloying elements dissolved and/or formed new phases causing a variation in the

values of the coefficients of elasticity (elastic modulus, bulk modulus and shear modulus), Poisson's ratio and internal friction of Sn-5Sb-2Cu ,Sn-5Sb-2Cu-2Se, Sn-5Sb-2cu-2In and Sn-5Sb-2Cu-2Se-2In lead free bearing solder alloys are summarized in Table2. From this table it is obvious that, the elastic modulus and internal friction values of these alloys vary, which is depending on its alloys composition. It is found that the elastic moduli increases from 57.05 GPa for ternary alloy Sn-5Sb-2Cu to 67.79 GPa for penta Sn-5Sb-2Cu-2Se-2In alloy. It is due to high performance metal alloys and intermetallic particles such as $Sb_{0.21}Sn_{0.79}$, Cu_3Sn, Cu_3Sb and InSb which act as hard inclusions in the β-Sn matrix. It can be seen that the axial ratio c/a of β-Sn is expanded with the addition of Se and In. This means that the increases in axial ratio with Se and In content normally leads to increase elastic moduli of all studied alloys. Also, modification in the internal β-Sn matrix structural of these alloys due to the forming of inter-metallic particles such as $Sb_{0.21}Sn_{0.79}$, Cu_3Sn, Cu_3Sb and new inter-metallic phase InSb imbedded in β-Sn matrix, crystal structure (size, shape and position) of these phases, refine matrix structure and solid solution as explained by [1, 36].

The elastic constants of the metallic alloys for the fundamental physical properties especially the mechanical properties such as strength, plastic deformation and fracture were reported previously using single crystals [37]. The highest elastic modulus was obtained for the alloy containing Se and In at 2 wt. % level; this is due to formation of intermetallic particles $Sb_{0.21}Sn_{0.79}$, Cu_3Sn, Cu_3Sb and InSb. The presence of the hard phases (intermetallic particles, $Sb_{0.21}Sn_{0.79}$, Cu_3Sn, Cu_3Sb and InSb) in the β-Sn matrix gives the alloy its high strength. In real polycrystalline melt-spun alloys, other factors such as porosity, concentration of impurities, inter-granular phases and alloying elements may influence the magnitude of the elastic constants. It should be pointed out that the measurements of the elastic modulus is quite complicated for highly rate sensitive micro structurally evolving solution, porosity, the cross-section thickness , volume fraction of precipitates and may be sensitive to electron concentration. It is noted that in this study by the addition of Se and In at 2wt.% level the increase in elastic modulus is about 67.79 GPa.

Table 2: Internal Friction and Elastic Moduli for Rapidly Solidified Sn-5Sb-2Cu Based Bearing Lead Free Solders

Solder	Internal Friction (Q^{-1})	Young's Modulus (E) Gpa	Shear Modulus (G) Gpa	Bulk Modulus(B) Gpa	Poisson's Ratio (N)
Sn-5Sb-2Cu	0.054	57.05	20.66	54.11	0.3306
Sn-5Sb-2Cu-2Se	0.042	59.12	21.79	57.06	0.3306
Sn-5Sb-2Cu-2In	0.035	63.45	22.50	59.88	0.3330
Sn-5Sb-2Cu-2Se-2In	0.025	67.79	24.00	63.87	0.3330

Table 3: Vickers Hardness of Rapidly Solidified Sn-5Sb-2Cu Based Bearing Lead Free Solder Alloys at Fixed Dwell Time 5 S

Solder	H_v MPa Load = 0.098 N	H_v MPa Load = 0.245 N	H_v MPa Load = 0.49 N
Sn-5Sb-2Cu	255.02	245.01	223.23
Sn-5Sb-2Cu-2Se	329.45	319.74	310.96
Sn-5Sb-2Cu-2In	302.14	288.42	273.32
Sn-5Sb-2Cu-2Se-2In	395.27	392.22	372.21

Vickers Hardness and Indentation Creep

Micro-hardness measurement is a very sensitive to detect the microstructural changes of different soft solders. Usually, it is a non-destructive testing and can be the easiest way to determine the mechanical properties of the different phases of the structure. Table 3 shows the variation of Vickers hardness number of Sn-5Sb-2Cu based alloys using constant applied loads 0.098, 0.245 and 0.49 N for constant dwell time of 5 s. The hardness increases continuously after addition selenium or indium to Sn-5Sb-2Cu base alloy up to 395 MPa for Sn-5Sb-2Cu-2Se-2In. This is attributed to the presence of more intermetallic particles such as $Sb_{0.21}Sn_{0.79}$, Cu_3Sn, Cu_3Sb and InSb and refinement the grain size [1]. The addition of 2

wt.% Se or In to Sn-5Sb-2Cu improves hardness by refining the particle size where similar studies have been carried out by Hu *et al* [38] in the case of Ag or Au into Sn-0.7Cu. Also, incorporating intermetallic particles improves strength and hardness. Figure 2 shows the compositions of indentation creep curves at room temperature under constant stress levels 0.098, 0.245 and 0.49 N. It can be observed that at all testing loads there is a rather wide gap between the curves of the ternary Sn-5Sn-2Cu and the quaternary Se- or In-containing alloys while narrow gap for penta Sn-5Sb-2Cu-2Se-2In alloy. As this figure shows, the lower level and slope in the steady-state region belongs to the Sn-5Sb-2Cu-2Se-2In alloy and the highest to the Sn-5Sb-2Cu alloy, the other two materials lying in between. The observed differences in the impression creep behavior of the alloys can be attributed to their respective structures. In the indentation experiments the strains are not uniform. The creep curves, presented as the plots of indentation diagonal length (D) versus dwell time, at various constant loads for both rapidly solidified materials are shown in Figure 2. It can be seen that the curves consist of two stages similar to an ordinary creep curve.

The first stage of the curve records an increase in the concerned variable with time, with a decreasing rate, followed by a steady state region where indentation sizes increase linearly with time. It is also notable that the indentation creep behavior of both materials is affected by loads. As it can be observed, both the level and slope of indentation curves in the steady-state region raise as the testing loads increases. In the Mulhearn-Tabor method, the variation of hardness with dwell time is shown in a log-log scale in Figure 3. This figure shows that hardness decreases with increasing dwell time due to indentation creep. Furthermore, the hardness of both conditions measured at different loads can be represented as a linear function of time. The slope of the resultant lines according Mulhearn-Tabor method is – (n+1/2) from which it is possible to calculate the stress exponent n. The stress exponents calculated in this way are listed in Table 4. As the testing load increases from 10 gf to 50 gf, the values of the stress exponent decrease from 8.88 to 5.83 for the both rapidly solidified alloys.

The stress exponent values of Sn-5Sb-2Cu based alloys are given in Table 4. These exponent values are in the range 5.83-8.88 depending on the composition of used alloy and it agrees with the previous results. The slight scatter of the data obtained at different loads may be attributed to the change in the structure during the indentation creep measurements. It can be seen that there is generally a good agreement between these stress exponents and those obtained from [10]. In the low stress range (from 10 to 50 gf) it is characterized by n values of 5.83-8.75, while at high stress range, n is approximately equal to 5.95-8.88. This means that the stress exponent becomes stress dependent for the four alloys. It should be emphasized here that such values of n are comparable to those of n values of 5.5-9.8 at 27-100 C for Sn-8.1Sb and 5-7.6 at 23-150 ˚C for Sn-5Sb [39, 40]. Therefore, the rapidly solidified alloys with significantly higher n values are more resistant to impression creep compared to the wrought material showing n values of 2.8 [11]. The change in stress exponent values are attributable to micro-structural features, changes in β-Sn matrix, such as the change in the lattice parameters, solid solution, size and distribution of strengthening phases, intermetallic particles agree with the results in [41].

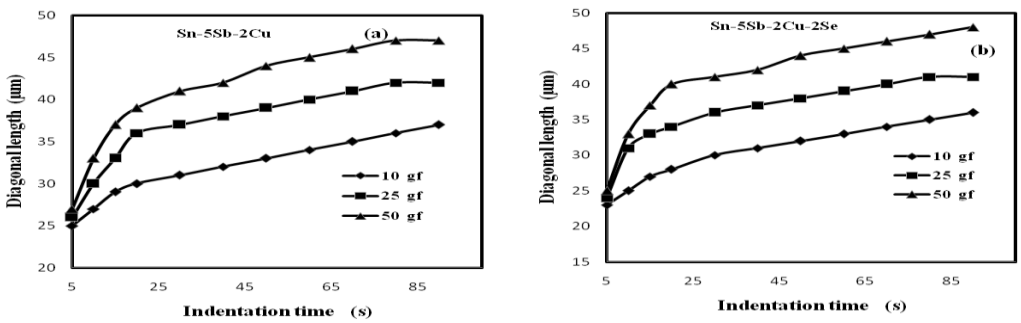

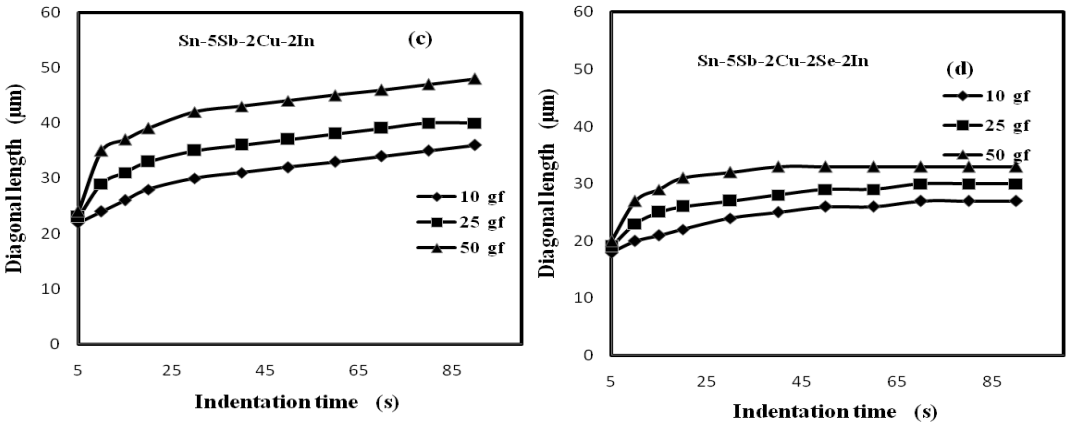

Figure 2: Indentation Creep Curves for the Rapidly Solidified Sn-5Sb-2Cu Based Alloys at Different Loads

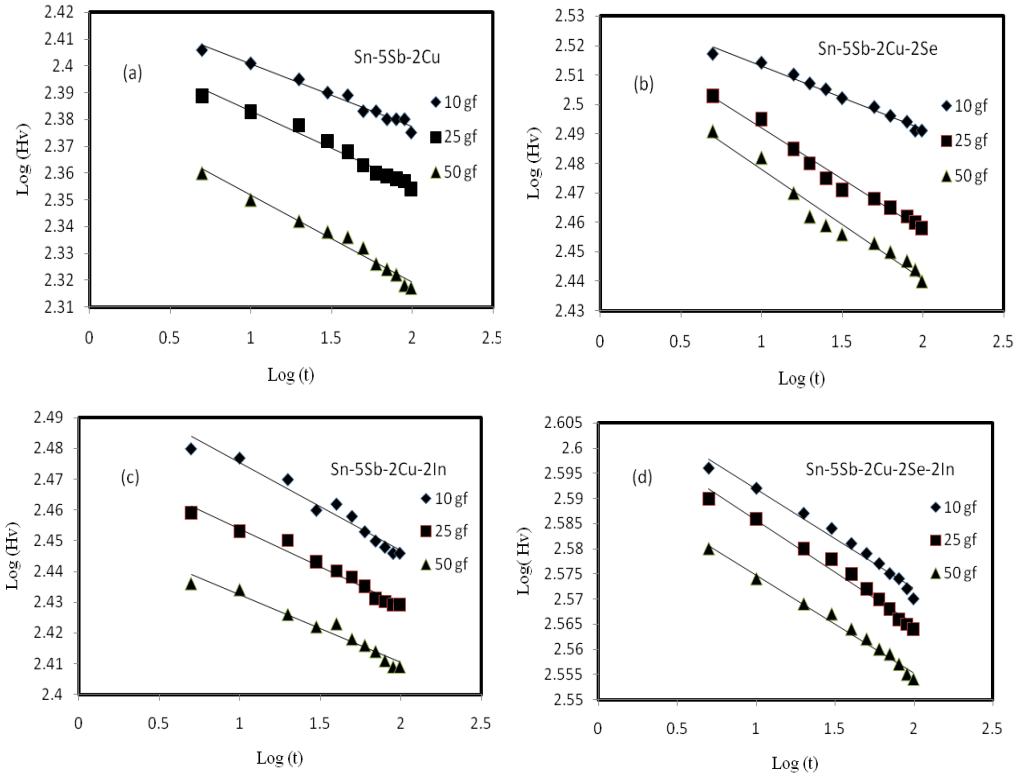

Figure 3: Hardness-Dwell Time Log-Log Plots for Rapidly Solidified Materials at Different Loads. The Slope of these Lines will be – (n+1/2) from the Stress Exponent, n, is Determined

Table 4: Materials Characteristics and Stress Exponents Derived from Mulhearn-Tabor Model

Condition	Solder	Load (gf)	Stress Exponent (n)
Melt-spun	Sn-5Sb-2Cu	10	5.83
		25	5.90
		50	5.95
Melt-spun	Sn-5Sb-2Cu-2Se	10	6.95
		25	6.11
		50	6.23
Melt-spun	Sn-5Sb-2Cu-2In	10	7.83
		25	7.92
		50	7.01
Melt-spun	Sn-5Sb-2Cu-2Se-2In	10	8.75
		25	8.82
		50	8.88

CONCLUSIONS

This paper has investigated the influences of Se and In on structure, mechanical properties and indentation creep of Sn-5Sb-2Cu based lead-free bearing solder alloys. The results are summarized as follows:

- Effect of Se and In on the mechanical response of Sn-Sb-Cu solder studied. Se and In addition made fine particles of IMCs with more uniform distribution. These fine IMC particles have made the solder to be strong and more ductile.
- From XRD examination, the tetragonal $Sb_{0.21}Sn_{0.79,}$ hexagonal Cu_3Sn and cubic Cu_3Sb intermetallic compounds are precipitated within the β-Sn matrix in the Sn-5Sb-2Cu lead free bearing solder alloys. The quaternary Sn-5 Sb-2Cu-2In and penta Sn-5Sb-2Cu-2Se-In alloys exhibited additional constituent phases of new cubic IMC InSb.
- The Sn-5Sb-2Cu-2Se-2In lead-free bearing solder proved to be promising in that it gave good combination of higher creep resistance and mechanical properties than the other three alloys, which was possible mainly due to existence of $Sb_{0.21}Sn_{0.79,}$ Cu_3Sn, Cu_3Sb and InSb IMCs. Also, rapid solidification and small addition of Se and In content leads to formation of new inter-metallic particles and a refined the particle size.
- The stress exponent n-values calculated from different methods of analysis are in good agreement with each other. The obtained stress exponents, which decreased with increasing stresses, were found to be 5.83-8.75 at low stresses and 5.95-8.88 at high stresses for Sn-5Sb, Sn-5Sb-2Cu, Sn-5Sb-2Cu-2Se and Sn-5Sb-2Cu-2Se-2In.

REFERENCES

1. R.M.Shalaby, J.Alloys Comp. 480 (2009) 334-339.
2. A.A.El-Daly, Y.Swilem, A.E.Hammad, J.Alloys Compd. 471 (2009) 98-104.
3. R.Novakovic, D.Giuranmo, E.Ricci, S.Delsante, D.Li, G.Borzone, Surface Sci.605 (2011) 248-255.
4. K.L.Murty, F.M.Haggag, R.K.Mahidhara, J.Electron.Mater.26 (1997) 839.
5. J.Yu,D.K.Joo,S.W.Shin, Acta Mateter.50 (2002)4315.
6. R.J.McCable, M.E.Fine, Metall.Mater.Tran A33 (2002)1531.
7. H.Mavoori, Jom 52(2000)29.
8. A.De La Torre, P.Adeva, M.Aballe,J.Mater.Sci, 26 (1991)4351.
9. G.Sharma, R.V.Ramanajan, T.R.G.Kutty, G.P.Tiwari, Mater. Sci. Eng, A278 (2000) 106.
10. R.Mahmudi, A.R.Geranmayah, M.Bakherad, M.Allami, Mater. Sci. Eng.A 457(2007)173-179.
11. R.Mahmudi, A.R.Geranmayeh, a.Razaee-Bazzaz, Mater. Sci. Eng, A, 448 (2007)287-293.
12. A.R.Germayayeh, G.Nayyeri, R.Mahmudi, Mater. Sci. Eng, A 547 (2012)110-119.
13. M.Kerr, N.Chawla, JOM 65 (2004) 50.
14. D.Joo, J.Yu, S.Shin, J.Electron.Mater, 32 (2003) 541.
15. M.Mathew, H.Yang, S.Movva, K.Murty, Metall, Mater.Tran.36A (2005) 99.
16. R.McCabe, M.Fine, Metall.Mater.Trans.33A (2002)1982.

17. R.McCabe, M.Fine, J.Electron.Mater.31 (2002) 1276.
18. N.Wade, K.Wu, J.Kunii, S.Yamada, K.Miyahara, J.Electron.Mater, 30 (2001) 1228.
19. M.D.Mathew,H.Yang,S.Movva, K.L.Murty, Metall.Mater.Trans.A36 (2005)99.
20. F.Ochoa, X.Deng, N.Chawala, J.Electron.Mater.33 (2004)1596.
21. R.A.Islam, B.Y.Wu,M.O.Alam, Y.C.Chan, W.Jillek, J.Alloys.Compd.392(2005)149.
22. R.Mahmudi, A.R.Geranmayeh, M.Allami, M.Bakherad, J.Electron.Mater. 36 (2007) 1703-1710.
23. R.K.Mahidhara, S.M.L.Sastry, I.Turlik, K.L.Murty, Scripta Metall. 31(1994) 1145-1150.
24. A.El-Bediwi, A.R.Lashin, M.Mossa, M.Kamal, Mater. Sci. Eng.A, 528 (2011)3568-3572.
25. A.A.Eldaly, A.Z.Mohamed, A.Fawzy, A.M.El-Taher, Mater. Sci. Eng, A 528(2011) 1055-1062.
26. F.Yang, J.C.M.Li, Mater.Sci.Eng.A 201(1995)40-49.
27. A Rezaee-Bazzaz, R.Mahmudi, Mater. Sci. Technol, 21(2005)861-866.
28. R.Mahmudi, A.R.Gernmayeh,H.Noori, N.Jahangiri, H.Khanbareh, Mater. Sci. Eng, A 487(2008) 20-25.
29. R.Mahmudi, A.R.Geranmayeh, H.Noori, M.Shahabi, Mater. Sci. Eng, A 491 (2008)110-116.
30. S.N.G.Chu, J.C.M.Li, J. Mater.Sci.12 (1977)2200-2208.
31. F.Kabirian, R.Mahmudi, Metall.Mater.Trans.A 41A (2010)3488-3498.
32. E.Schriber, O.L.Anderson, N.Soga, Elasatic Constant and their measurements, McGraw-Hill, New York, 1973, pp.82.
33. S.Timoshenko, J.N.Goddier, Theory of Elasticity, 2nd ed., McGraw Hill, New York, 1951, pp. 277.
34. R.M.Shalaby, Mater. Sci. Eng.A 560 (2013)86-95.
35. T.O.Mulhearn, D.Tabor, J.Inst, Metals 89 (1960)7.
36. R.M.Shalaby, J. Alloys and Compd. 505 (2010) 113-117.
37. M.Nakamura, K.Kimura, J.Mater.Sci.26 (1991) 2208-2214.
38. Huh SH, Suganuma K, Oku T, Inoue M.Proc 6th symposium on microjoining and assembly technology in electronics, Yokohama: Japan Welding Society, 2000, pp 229-32.
39. S.Choi, J.Lee, F.Guo, T.Bieler, K.Subramanian, J.Lucas, JOM 53(2001)22.
40. M.Huang, C.Wu, L.Wang, J.Electron.Mater.34 (2005) 1373.
41. S.Deraki Rani, G.S.Murthy, Mater.Sci.Technol, 403 (2004)20.